



BNL-105177-2014-TECH

Booster Technical Note No. 133;BNL-105177-2014-IR

# REPORT ON THE TEST AND MEASUREMENT OF THE FAST KICKER SYSTEM

W. Zhang

December 1988

Collider Accelerator Department  
**Brookhaven National Laboratory**

**U.S. Department of Energy**

USDOE Office of Science (SC)

Notice: This technical note has been authored by employees of Brookhaven Science Associates, LLC under Contract No.DE-AC02-76CH00016 with the U.S. Department of Energy. The publisher by accepting the technical note for publication acknowledges that the United States Government retains a non-exclusive, paid-up, irrevocable, world-wide license to publish or reproduce the published form of this technical note, or allow others to do so, for United States Government purposes.

## **DISCLAIMER**

This report was prepared as an account of work sponsored by an agency of the United States Government. Neither the United States Government nor any agency thereof, nor any of their employees, nor any of their contractors, subcontractors, or their employees, makes any warranty, express or implied, or assumes any legal liability or responsibility for the accuracy, completeness, or any third party's use or the results of such use of any information, apparatus, product, or process disclosed, or represents that its use would not infringe privately owned rights. Reference herein to any specific commercial product, process, or service by trade name, trademark, manufacturer, or otherwise, does not necessarily constitute or imply its endorsement, recommendation, or favoring by the United States Government or any agency thereof or its contractors or subcontractors. The views and opinions of authors expressed herein do not necessarily state or reflect those of the United States Government or any agency thereof.

**REPORT ON THE TEST AND MEASUREMENT  
OF THE FAST KICKER SYSTEM**

**AD  
BOOSTER TECHNICAL NOTE  
NO. 133**

**W. ZHANG, J. BUNICCI, W. FREY and A. SOUKAS  
DECEMBER 22, 1988**

**ACCELERATOR DEVELOPMENT DEPARTMENT  
BROOKHAVEN NATIONAL LABORATORY  
UPTON, NEW YORK 11973**

# Report on the Test and Measurement of the Fast Kicker System

*Wu Zhang, John Bunicci, Walter W. Frey, and Anastasios V. Soukas*

## I - INTRODUCTION

This report summarizes the primary test and measurement results of the pulsed power supply system of fast kicker magnets and the comparison of the actual system versus the calculated performance. The calculations are performed via computer-aided simulation of the ideal system, i.e., ideal circuit elements with nondistributed parameters. The purpose of this report is to evaluate, based on present knowledges, the existing technical difficulties, estimate the possible effects of the distributed circuit parameters and parameter variations of the nonideal circuit elements, etc. In addition the report attempts to provide some reasonable design considerations for Booster extraction and AGS injection systems. Some computer aided circuit analysis of the observed system phenomena are also included.

The major part of the report will discuss the system stray inductance, the effect of stray capacitance, the effect of series inductance of the

capacitors, and components measurement.

A general simplified or idealized circuit of a fast kicker pulsed power discharged circuit is shown in Figure 1.

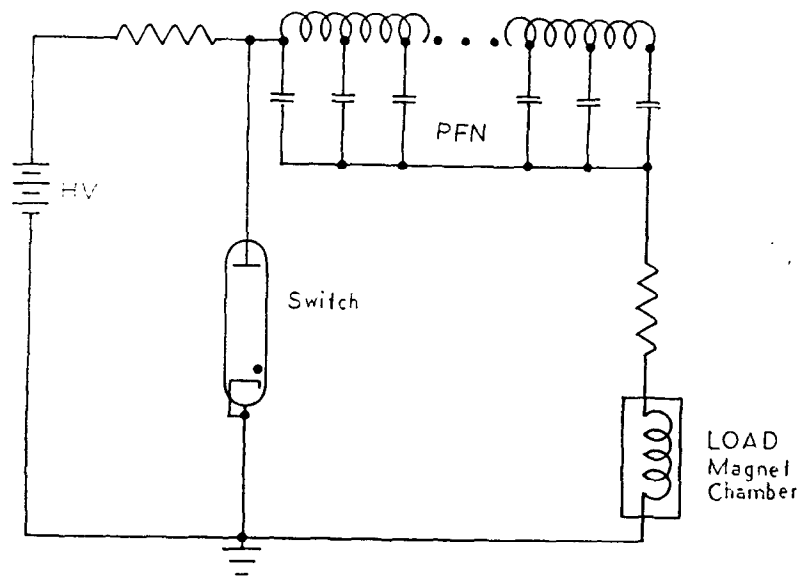


Figure 1

## II - SYSTEM STRAY INDUCTANCE

The system stray inductance in the pulsed power supply unit of kicker magnet includes:

1. External loop inductance,
2. Stray inductance of the switch -- thyatron tube,
3. Stray inductance inside the magnet chamber -- feed-through and internal conductor loop inductance.
4. Series inductance of capacitors.

For fast rise-time pulsers the total discharge inductance must be kept as low as possible. When the loop inductance of the magnet is in the order of  $1 \mu H$ , the stray circuit inductances become a significant part of the discharge circuit and can no longer be ignored. On electrical engineering consideration, the possible efforts that can be applied are to reduce the loop inductance, and to use low inductive elements.

### A - Magnet Inductance

The stray inductance inside the magnet chamber has been shown to be a big factor of the total stray inductance. The series resonance method has been used to measure the total inductance of the AGS H-5 and E-5 magnets inside their vacuum chambers. The measurement setup is shown in Figure 2.

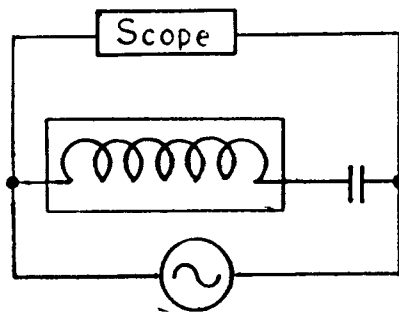


Figure 2

The capacitor used in the test is a vacuum capacitor with the following parameters:

$$C = 0.75 \text{ nf}$$

$$L_c = 37.4 \text{ nh} \quad (\text{series inductance of the capacitor})$$

The external lead is minimized to a length less than 1 *inch*, thus the inductance of the lead is small enough to be neglected. The inductance is determined from the resonant frequency  $f_o$  by using equation

$$L = \frac{1}{4\pi^2 f_o^2 C}$$

The measurement results are as follows:

H-5 magnet:

$$f_o = 5.6 \text{ MHz}$$

$$L_1 = 1080 \text{ nh}$$

$$L_{H-5} = L_1 - L_c = 1043 \text{ nh}$$

E-5 magnet:

$$F_o = 5.43 \text{ MHz}$$

$$L_2 = 1143 \text{ nh}$$

$$L_{E-5} = L_2 - L_c = 1106 \text{ nh}$$

The mechanical design of the H-5 and E-5 magnets is normally the same but they are connected in opposite polarities. The internal structure of the H-5/E-5 magnet is such that the two C-type ferrite magnet blocks are electrically in parallel and magnetically in series. Based on the parameters shown in drawing D-11-M-10820 (Magnet Block Drawing), we calculate the inductance of H-5/E-5 magnet as:

$$\begin{aligned} L_{block} &= \frac{4\pi w(l_m + 1.5h)}{10^9 h} \\ &= \frac{4\pi \times 3.6525 \times (43.18 + 1.5 \times 1.4376)}{10^9 \times 1.4376} \\ &= 1447.468 \text{ nh} \end{aligned}$$

where

$$h = 2 \times 0.283 \text{ inch} = 1.43764 \text{ cm}$$

$$w = 1.438 \text{ inch} = 3.65252 \text{ cm}$$

$$l_m = 17 \text{ inch} = 43.18 \text{ cm}$$

Thus, we have the magnet inductance as

$$L_{magnet} = \frac{1}{2} L_{block} = 723.734 \text{ nh} .$$

Comparing with the measured values of the H-5 and E-5 magnets, the difference is assumed to be stray inductance.

$$\Delta_{H-5} = L_{H-5} - L_{magnet} = 319.266 \text{ nh}$$

$$\Delta_{E-5} = L_{E-5} - L_{magnet} = 382.266 \text{ nh}$$

The ratio of the stray inductance to the designed value can be calculated as

$$\frac{\Delta_{H-5}}{L_{magnet}} = \frac{319.266}{723.734} = 44.11\%$$

$$\frac{\Delta_{E-5}}{L_{magnet}} = \frac{382.266}{723.734} = 52.82\% .$$

### B - External Loop and Switch Tube Stray Inductances

In the test circuit, we have tried to reduce the external loop inductance by making the mechanical connectors between the load magnet and the pulse forming network unit, and between the switch tube and the pulse forming network, as close as possible; using thicker connectors; and constructing the thyatron in a coaxial structure, etc. However, high voltage circuits always require a certain amount of spacing to avoid arcing, and this limits the further reduction of the external loop inductance.

The total system inductance has been measured by using single capacitor discharge method. The test setup is shown in Figure 3.

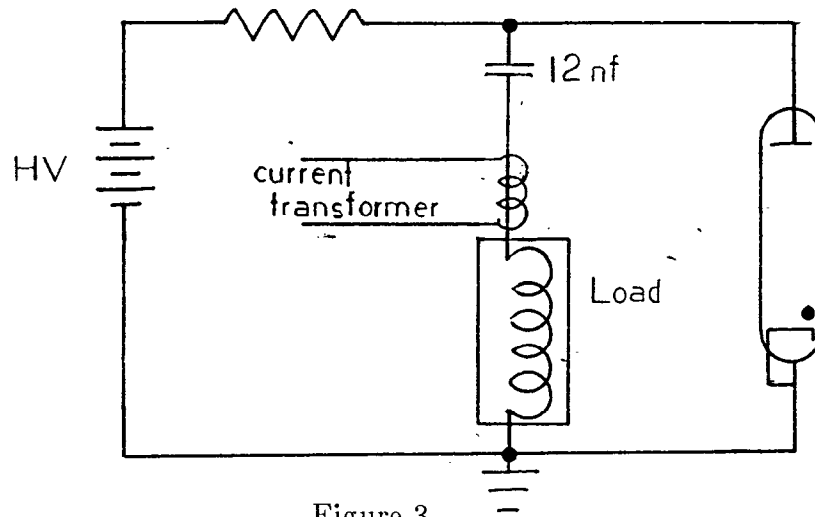


Figure 3

The load is the H-5 magnet, the capacitor has the following parameters:

$$C = 12.00 \text{ nf}$$

$$L_c = 121 \text{ nh}$$

The time of measured half sine wave is ( see Figure 4 )

$$\frac{T}{2} = 413 \text{ ns}$$

Thus, the total system inductance can be determined as

$$L_{total} = \frac{T^2}{4\pi^2 C} = 1440.18 \text{ nh}$$

The total stray inductance is

$$L_{stray} = L_{total} - L_{magnet} = 1440.18 - 723.734 = 716.45 \text{ nh} .$$

The ratio of stray inductance to the magnet design value and the ratio of total inductance to the magnet design value are:

$$\frac{L_{stray}}{L_{magnet}} = \frac{716.45}{723.73} = 99\%$$

$$\frac{L_{total}}{L_{magnet}} = \frac{1440.18}{723.73} = 199\% .$$

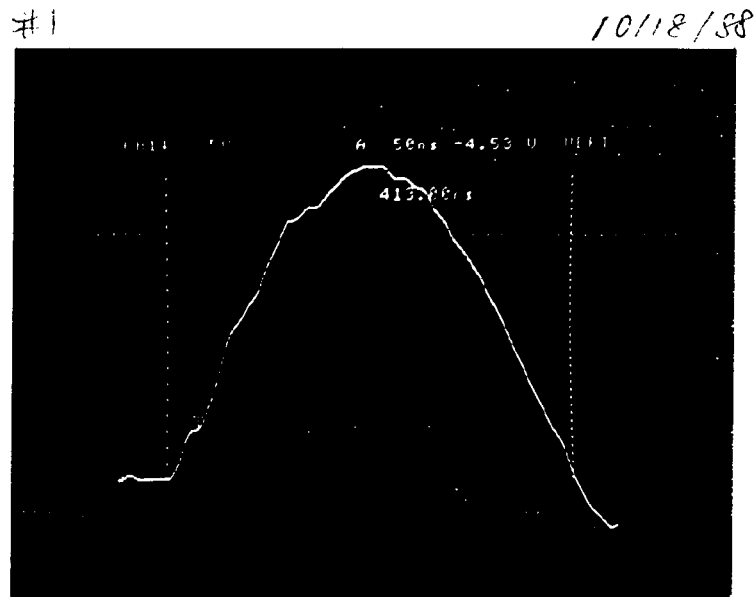


Figure 4  
Photograph of current discharge in circuit of Figure 3.

Remark: Consider that

$$L_{stray} = L_{i-loop} + L_{feed-through} + L_{e-loop} ,$$

where  $L_{i-loop}$  ( $L_{e-loop}$ ) is the internal ( external ) conductor loop stray inductance and  $L_{feed-through}$  is the feed-through stray inductance. Since the parallel connection of the two magnet blocks, the stray inductance due to the internal conductor loop of each magnet block could be twice of  $L_{i-loop}$ .

### **C - AGS Injection and Booster Extraction Kicker System Inductance Estimations**

Based on the above measurement results, we can estimate the total inductance of each section of the AGS injection kicker system and Booster extraction kicker system as follows:

AGS Injection Kicker System

$$w = 12.7 \text{ cm}$$

$$h = 5.7 \text{ cm}$$

$$l_m = \frac{101.6}{3} = 33.867 \text{ cm (3-sections)}$$

$$l = L_m + 1.5h = 42.417 \text{ cm}$$

$$\begin{aligned} L_{magnet} &= \frac{4\pi wl}{10^9 h} \\ &= \frac{4\pi \times 12.7 \times 42.417}{10^9 \times 5.7} = 1187.62 \text{ nh} \end{aligned}$$

$$L_{total} \geq L_{magnet} + L_{stray} = 1904.07 \text{ nh}$$

Booster Extraction Kicker System

$$w = 14 \text{ cm}$$

$$h = 7 \text{ cm}$$

$$l_m = \frac{228.6}{4} = 57.15 \text{ cm (4-sections)}$$

$$l = l_m + 1.5h = 67.65 \text{ cm}$$

$$L_{magnet} = \frac{4\pi \times 14.0 \times 67.65}{10^9 \times 7} = 1700.23 \text{ nh}$$

$$L_{total} \geq L_{magnet} + L_{stray} = 2416.68 \text{ nh}$$

Remark: As the reason explained in the last section, if the magnet of each section consists of a single block C-type magnet the loop stray inductance could be doubled. Therefore the total stray inductance is greater than the values shown above.

#### **D - Series Inductance of Pulsed Capacitors**

The pulsed capacitors used in the test circuit were a type especially designed for pulsed applications. We have measured the series inductance of different types of capacitors, and the results are listed in Table 1. Notice that the series inductance of the capacitor depends upon the rated voltage - which is usually proportional to the mechanical length of the capacitor, terminal construction, and the internal configuration of the

capacitor. The capacitors tested have different nominal ratings and use different materials, so that the absolute comparison is not adequate in that sense.

Table 1

MFG	Dielectric	Part #	Nominal Cap	Series Ind	Volt Rating
AXEL	dry mica	MD2BY253K	25 nf	112 nh	25 kv
STANLEY	recon mica	ZD802C403	2X20 nf	39.0 nh	8 kv
				38.5 nh	
		ZD802C403	2x20 nf	39.4 nh	8 kv
				32.0 nh	
SPRAGUE	?	W2409	7.5 nf	356.0 nh	60 kv
	ceramic	30DK-TS	0.5 nf	16.0 nh	30 kv
JENNINGS		CFSC-1250-15DE354	1.2 nf	81.5 nh	15 kv
		CFED-750-158	0.7 nf	41.5 nh	
		RFC-80-60	80 pf	80.0 nh	
CONDENSER	oil filled	KMSCR 123-40MX	12 nf	121 nh	50 kv
		KMSCR 123-40MX	12 nf	150-154 nh	50 kv
		KMSCR 502-40MX	5 nf	188 nh	50 kv
MAXWELL	oil filled	33799	200 nf	167 nh	80 kv
		33682	19 nf	80 nh	50 kv

### III - SYSTEM STRAY CAPACITANCE

#### A - Effect of Stray Capacitance

The major sources of stray capacitance in the circuit of Figure 1 are:

1. Inside the magnet chamber,
2. Between the pulse forming network common plate and the ground plate,
3. Capacitor cases to the thyatron cathode plate.

There are other sources of stray capacitance in the circuit, some are located between each turn of the PFN coils, some in the switch tube, etc. Depending on its magnitude, stray capacitance will have a variety of effects in the circuit performance. The major difficulty encountered in the test was the flat top ripple caused by stray capacitance. The photographs in Figures 5 and 6 show typical cases, which has the ripple level around +15% to -10%. The photograph of Figure 7 shows a comparison of the current waveforms obtained from a dummy load - air coil, and from the real load - H-5 magnet. The top trace is the current waveform of the coil, and the lower trace is the current waveform of the H-5 magnet ( the magnet chamber was grounded ). This comparison indicates that the stray capacitance inside the magnet chamber is the main factor of the ripple level. This effect can also be shown by computer simulation. The computer results are shown in Figures 8 and 9, which show the schematic diagram and results thereof, respectively.

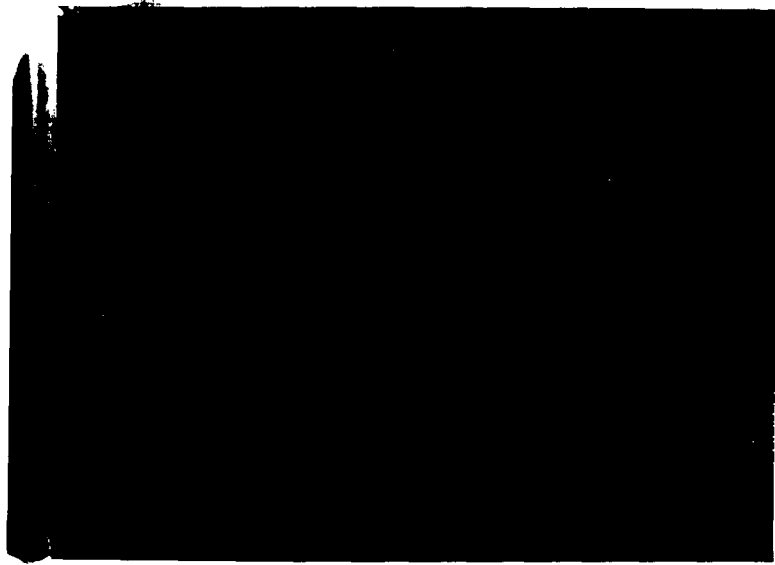


Figure 5

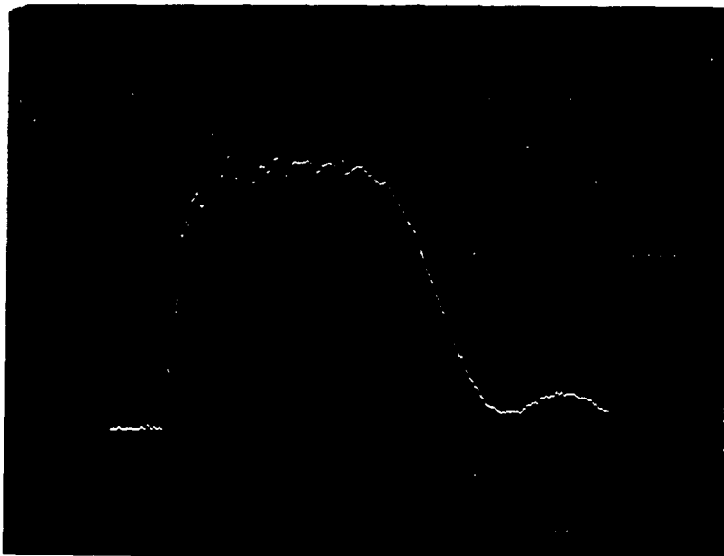


Figure 6

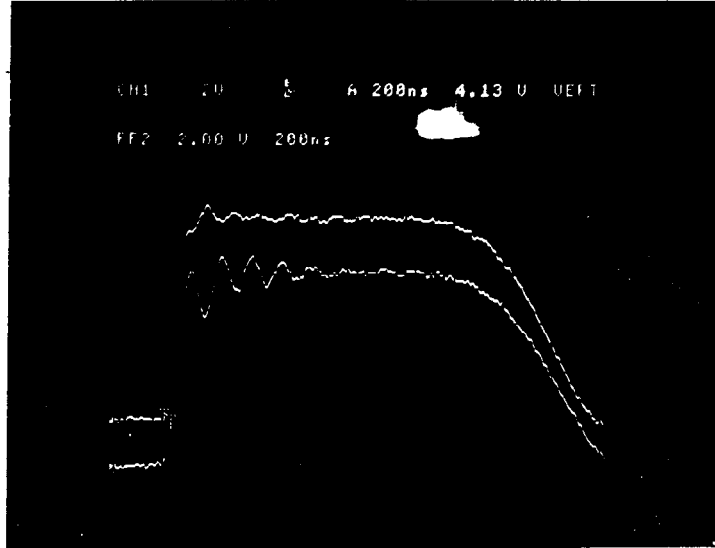


Figure 7

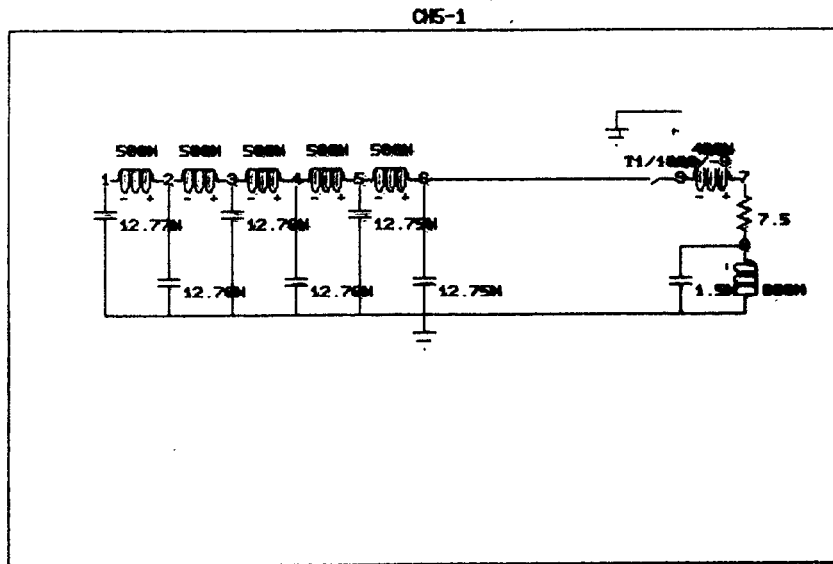


Figure 8

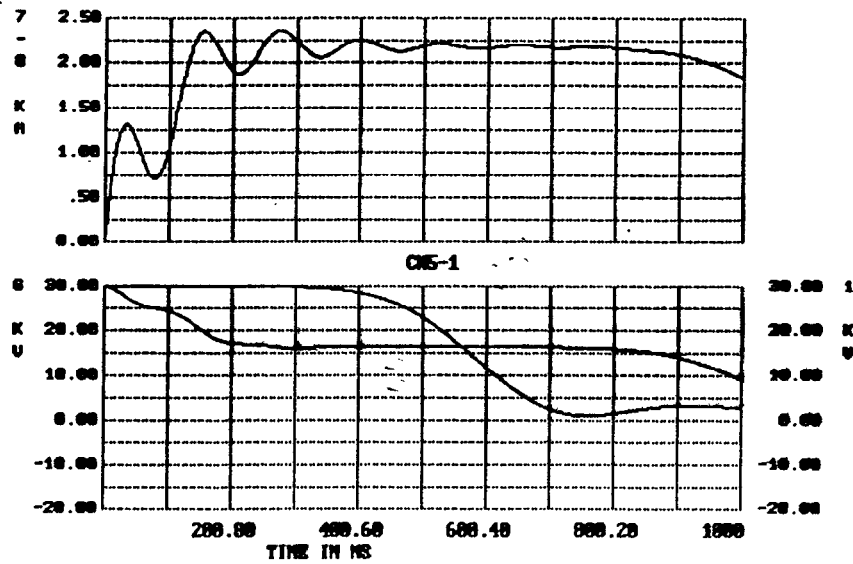


Figure 9

## B - Methods Applied to Reduce the Ripple Level

To reduce the flat top ripple level, we have tried to:

1. float the vacuum chamber through a  $116\text{ohm}$  resistor to ground, which could dampen the ripple faster, but the remaining ripples still would be high enough to hurt the flat top, and bring the vacuum chamber to a high voltage during the transient;
2. use a high pass filter to bypass the high frequency ripple, which also bypasses the high frequency components needed to get fast rise time ( see photograph of Figure 10 );
3. change PFN parameters, which is based on the simulation and experiment that slower rising long section pulse could have smaller ripples;
4. Increase the inductance value, which would slow down the pulse rise time.

It is very clear that the pulse response is a trade off between the pulse rise time and the flat top ripple level. The long cable between power supply and load could also help obtain a smooth top, but problems related to it are the slower rise time and mismatched load.

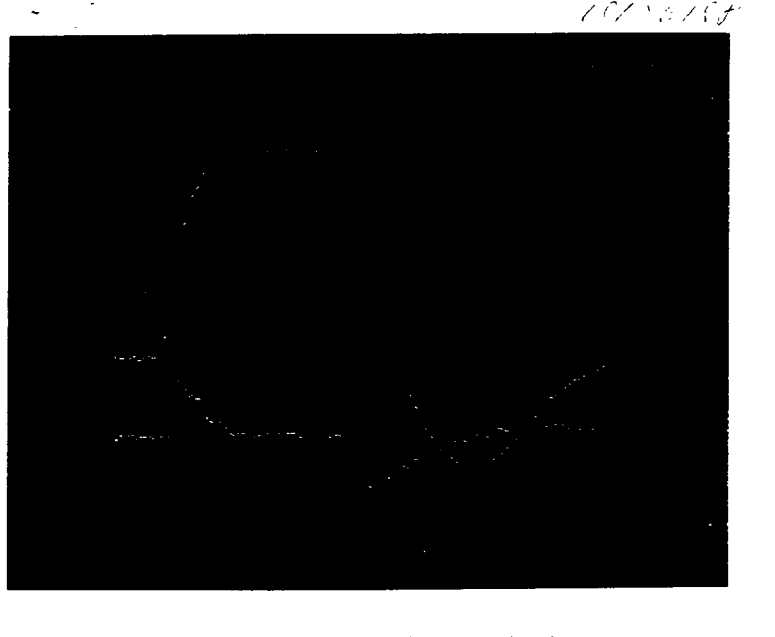


Figure 10

photograph of the waveforms of current pulse and current of by-pass filter.

#### IV - SERIES INDUCTANCE OF CAPACITOR AND MUTUAL INDUCTANCE OF COIL

Another difficulty encountered in the test is the overshoot on the fast rising part of the pulse. The photograph of Figure 11 is an example. This phenomenon is believed to be caused by the series inductance of the capacitor, the mutual inductance of PFN coils, and the stray capacitance of the circuit. This problem is somehow parameter dependent, i.e., it does not appear in the slower rising pulse.

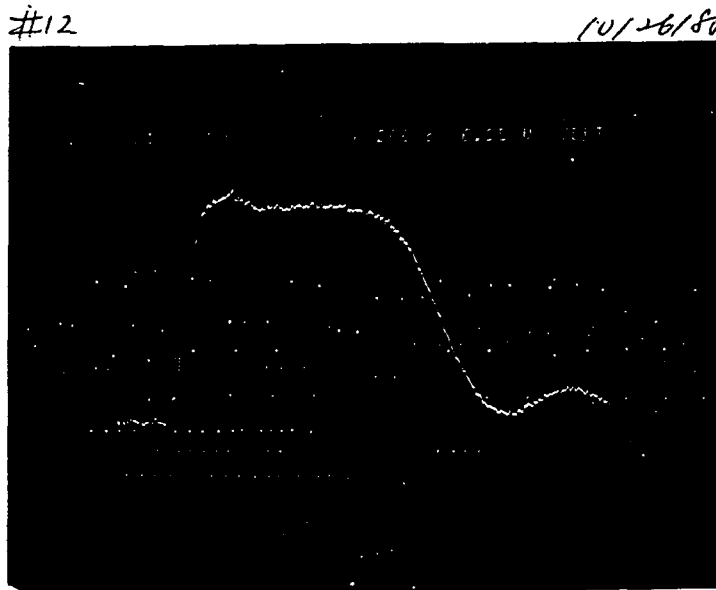


Figure 11

#### A - Capacitor Model

The circuit models of an ideal capacitor and an actual capacitor are given in Figures 12 and 13. Figure 14 is a simplified model of the

capacitor, showing the series inductance and omitting the resistors which represent losses. This circuit is more pertinent to our pulsed applications. Also capacitors have a wide tolerance from their nominal values. Table 2 shows some measurements of capacitors of a  $12\text{ nF}$  nominal capacitance value. If enough capacitors are available selections can be made to aid the pulse forming network design.

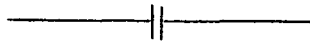


Figure 12 - ideal capacitor model

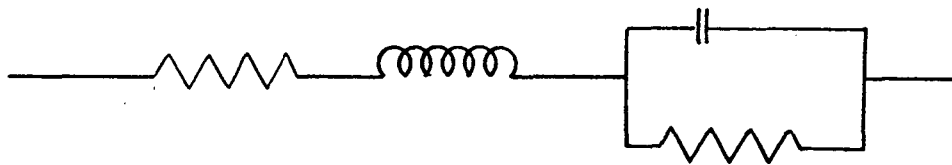


Figure 13 - actual capacitor model

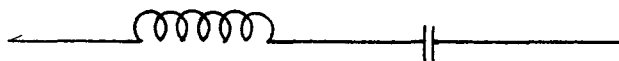


Figure 14 - simplified actual capacitor model

Table 2 - Nominal capacitance value 12 nF

#	Measured Value		#	Measured Value
1	12.77		14	12.00
2	12.70		15	12.16
3	12.64		16	11.99
4	12.76		17	12.17
5	12.76		18	12.75
6	12.71		19	12.70
7	12.70		20	12.08
8	12.71		21	12.12
9	12.05		22	12.66
10	12.00		23	12.07
11	12.09		24	12.75
12	12.08		25	12.76
13	12.11		26	12.67

### B - Mutual Inductance

The mutual inductance of the adjacent coils is usually space dependent. The tighter space of the coil results in higher values of the mutual inductance. The circuit model of the mutual inductance is shown in Figure 15.

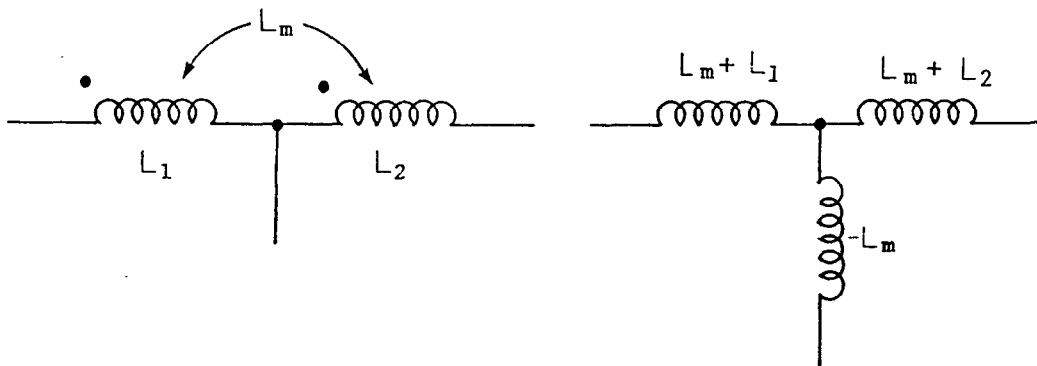


Figure 15

The circuit model of an ideal PFN, and the model including series inductance of the capacitors and the mutual inductance between the coils are given in Figures 16 and 17.

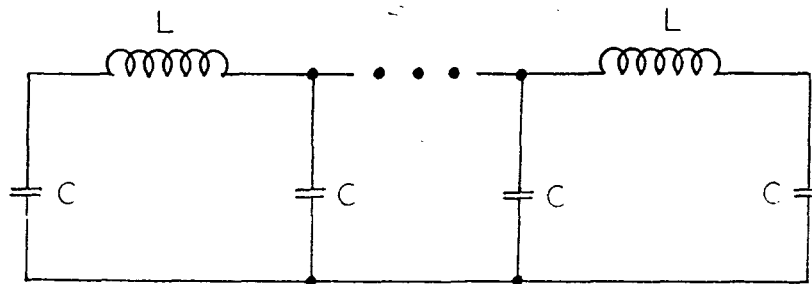


Figure 16

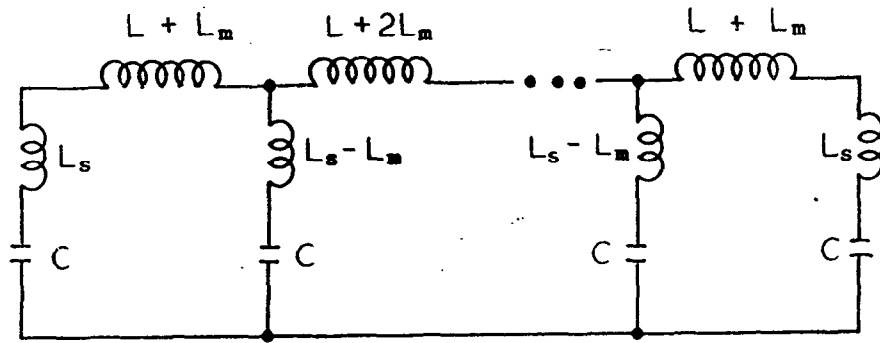


Figure 17

The Figures 18 - 21 are computer simulations of the circuit based upon the two different circuit models. The mutual inductance is assumed to be  $L_m = 60 \text{ nh}$  ( $78 \text{ nh}$ ), and the assumed series inductance of the capacitor is  $L_s = 120 \text{ nh}$ .

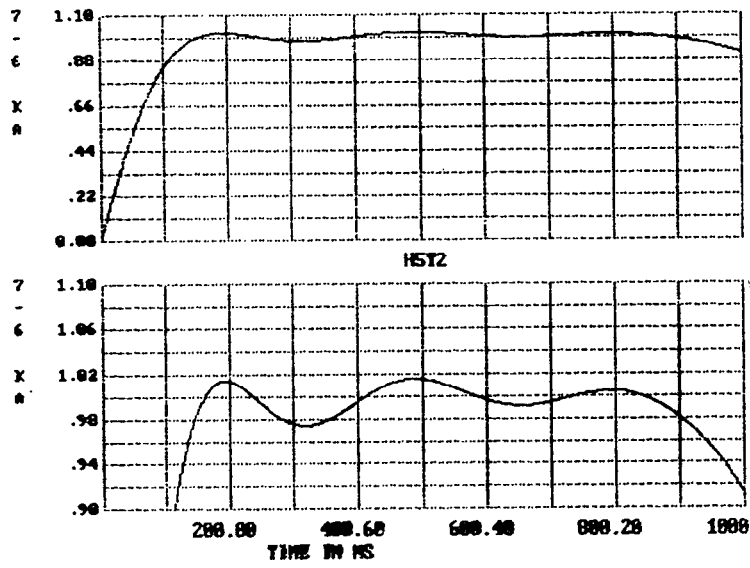
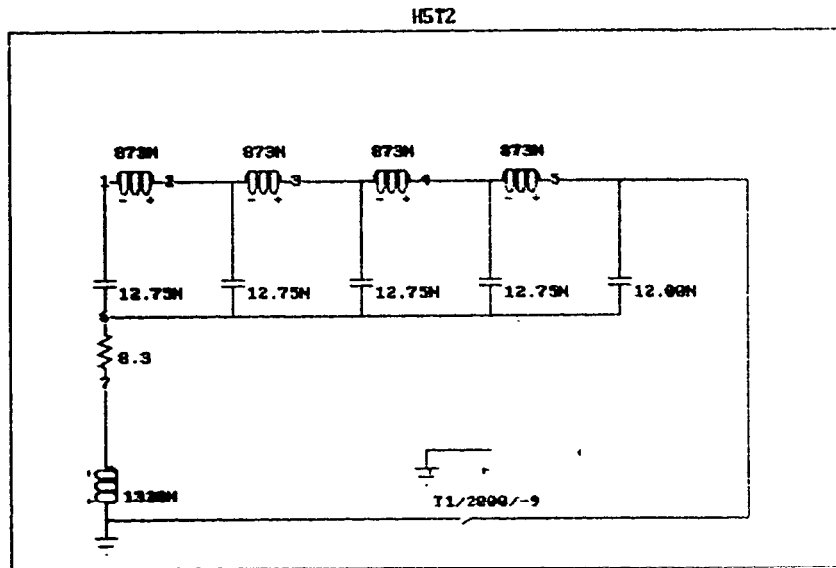


Figure 18

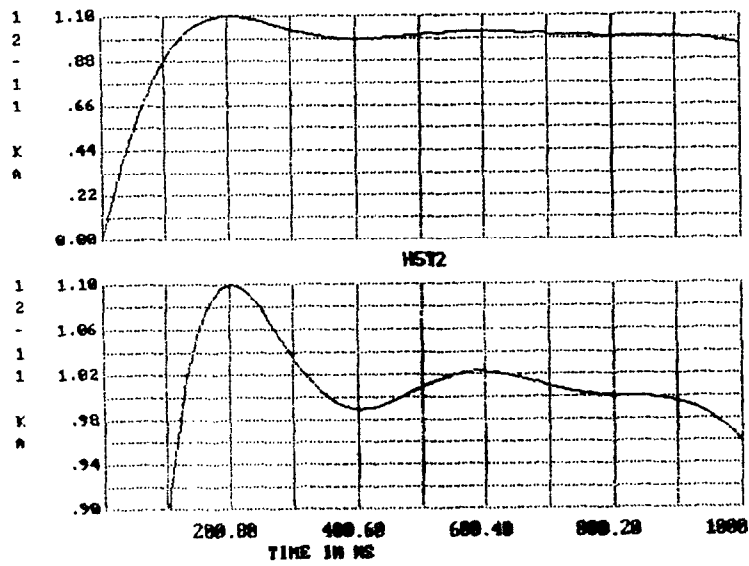
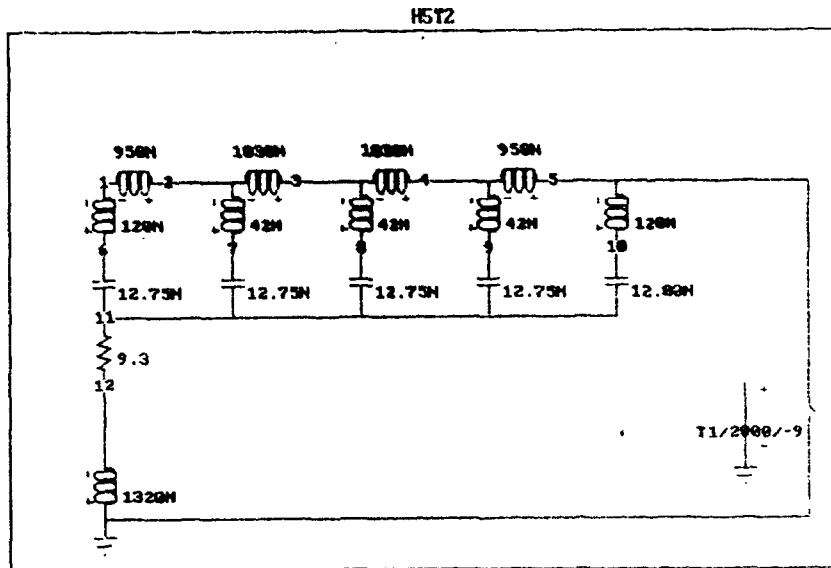


Figure 19

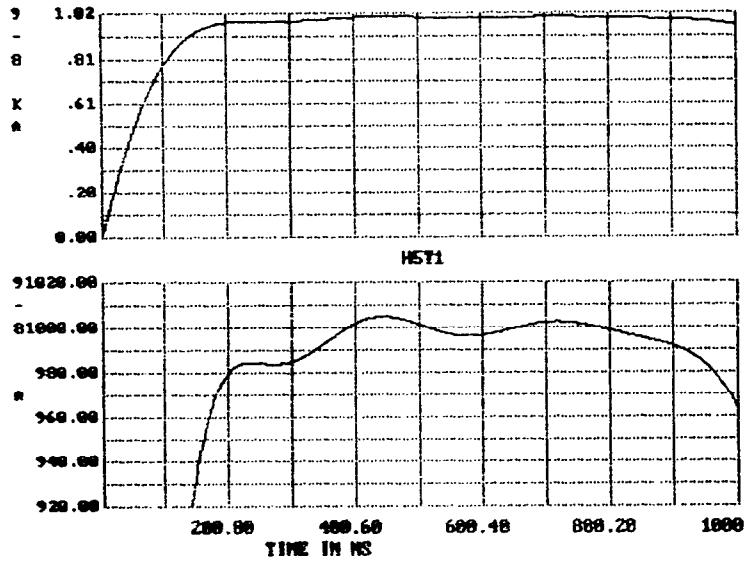
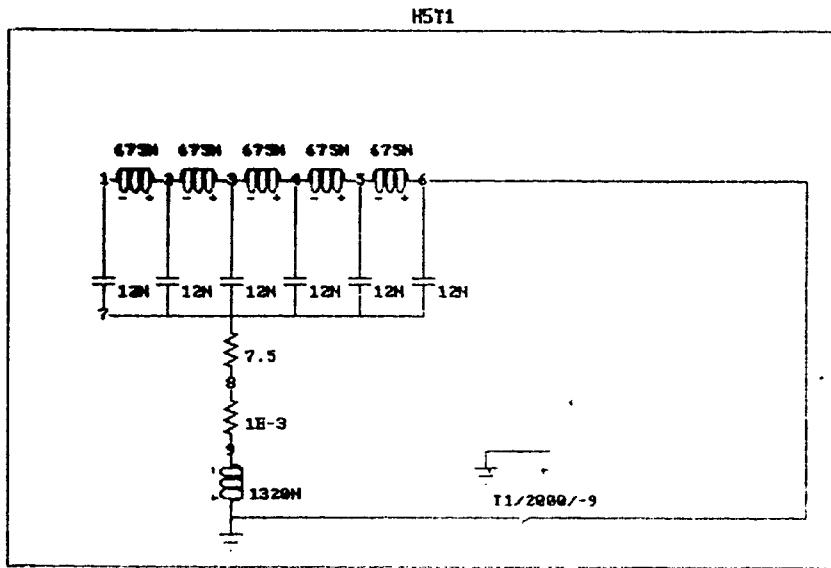


Figure 20

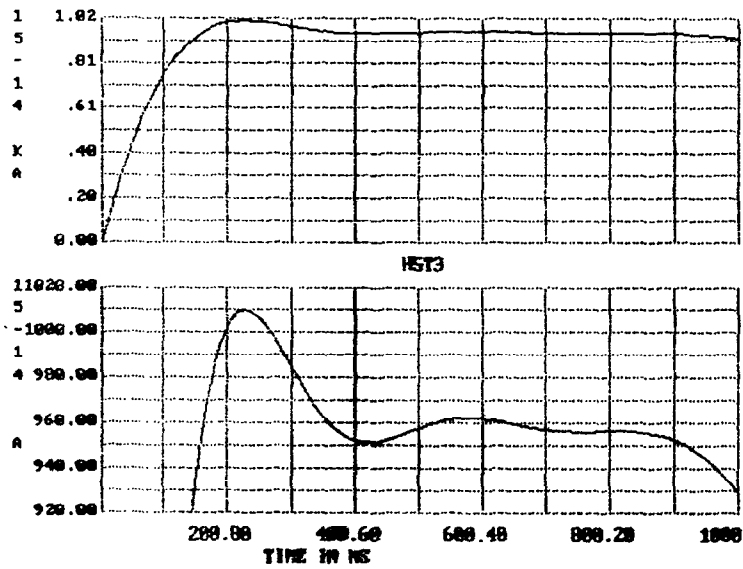
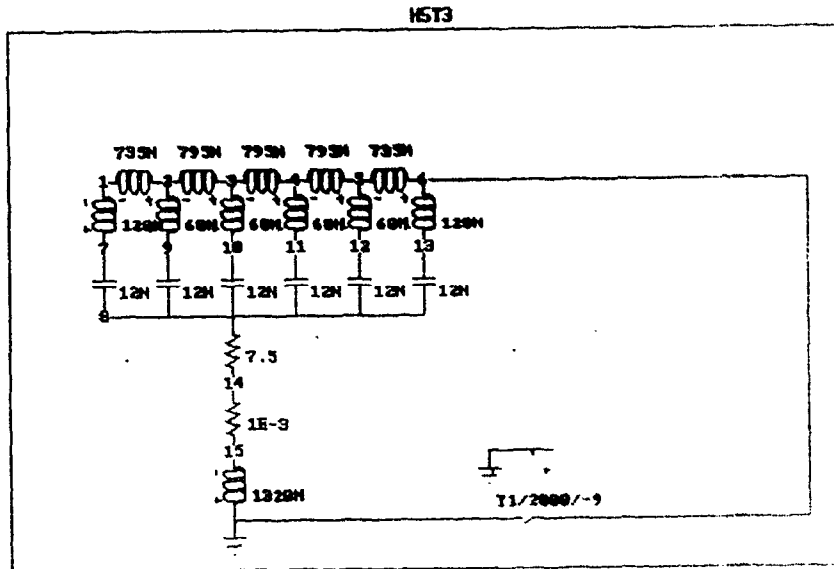


Figure 21

The comparison of the simulation shows that the overshoot is related to the series inductance of the capacitor and the mutual inductance of the coil. Reducing the overshoot is another trade off of the pulse rise time.

The Table 3 is attached as a reference, which shows the resistor tolerances from their nominal values.

Table 3 - Carborundum Resistors

#	Nominal Value	Measured Value
1	1.0	1.0
2	2.2	2.4
3	3.3	3.1
4	3.3	3.4
5	5.0	5.3
6	5.0	4.9
7	10.0	10.4
8	22.0	23.0